Contents lists available at ScienceDirect

### Progress in Oceanography

journal homepage: www.elsevier.com/locate/pocean



# Effects of the Kuroshio Extension jet and pinch-off ring on epipelagic mesozooplankton<sup>☆</sup>

Ruping Ge <sup>a</sup>, Hongju Chen <sup>a,b,\*</sup>, Yueqi Zhang <sup>c</sup>, Zhaohui Chen <sup>c</sup>, Facan Lei <sup>a</sup>, Weimin Wang <sup>a,d</sup>, Yunyun Zhuang <sup>a,b</sup>, Guangxing Liu <sup>a,b</sup>

- a Key Laboratory of Marine Environment and Ecology, Ministry of Education, Ocean University of China, Qingdao 266100, China
- b Laboratory for Marine Ecology and Environmental Science, Qingdao Marine Science and Technology Center, Qingdao 266237, China
- <sup>c</sup> Frontier Science Center for Deep Ocean Multi-spheres and Earth System (FDOMES), Physical Oceanography Laboratory, Ocean University of China, Qingdao 266100, China
- <sup>d</sup> Laoshan Laboratory, Qingdao 266237, China

#### ARTICLE INFO

Keywords: Kuroshio extension Pinch-off ring Epipelagic mesozooplankton Community structure Functional traits

#### ABSTRACT

The eastward flow of the Kuroshio Extension (KE) is accompanied by intense eddy activities at both the mesoscale and submesoscale levels, exerting a substantial effect on biogeochemical processes in the upper ocean. The present study focused on how the KE jet and pinch-off cyclonic eddy influenced mesozooplankton community structure and functional traits in the northwestern Pacific. The zooplankton communities in the investigated regions formed a four-segment pattern from north to south, with significant differences in the species and functional trait compositions of each group. The KE stream acted as a barrier that prevented water exchange between the Kuroshio-Oyashio mixed water (KOMW) and North Pacific Subtropical Gyre (NPSG) regions. A comparatively higher proportion of current-feeding omnivore-herbivore zooplankton was recorded in the NPSG region when compared to the KOMW and KE regions, which can be attributed to the influence of the pinch-off cyclonic eddy. Red Noctiluca scintillans was carried from the coast of Japan to open water by the KE's eastward advection, and it bloomed  $(1.2 \times 10^4 \, \text{ind} \cdot \text{m}^{-3})$  in the KOMW under favorable hydrological and nutritional environments, changing the community structure of zooplankton. The pinch-off cyclonic eddy could increase zooplankton abundance but had no significant impact on species composition and functional traits. In addition, the divergence effect of the eddy resulted in greater zooplankton abundance at its edges than in the center. This study enhanced our knowledge of the impacts of the KE on zooplankton communities and has significant implications for understanding pelagic plankton and nutrient responses to pinch-off mesoscale eddies.

#### 1. Introduction

The Kuroshio is a western boundary current in the North Pacific and one of the strongest ocean currents in the world. It reaches the Okinawa Trough via the Yonaguni Depression off the eastern coast of Taiwan Island, flows along the continental slope of the East China Sea, and then turns eastward through the Tokara Strait. After passing the area south of Japan, the Kuroshio separates from the coast of Japan at the Boso Peninsula to flow eastward into the North Pacific Ocean as a free jet—the Kuroshio Extension (KE; Qiu, 2002; Usui et al., 2013; Yang et al., 2022). The Kuroshio including KE transports tropical warm water with energy, nutrients, and organisms, as well as coastal water from southern Japan,

to the mid-latitudes, which can influence on the marine ecosystem in the northwestern Pacific (Chiba et al., 2009; Chiba et al., 2013; Nagai et al., 2019; Nagai et al., 2021; Nishikawa and Yasuda, 2011; Yamamoto et al., 1988).

The KE manifests as a zonal jet accompanied by large amplitude meanders and vigorous pinch-off eddies (Qiu, 2003). The pinch-off cyclonic eddies in the KE region frequently generate during spring, with the steady meander of the KE jet (around 144°-146°E) representing the area where it frequently appears (Ding et al., 2019). These pinch-off eddies, which carry various features associated with their source, can travel hundreds or even thousands of kilometers and have a life history that may last for months or even years (Hamilton et al., 2016; Lipphardt

https://doi.org/10.1016/j.pocean.2025.103523

<sup>\*</sup> This article is part of a special issue entitled: 'AMS-West Pac. and changes' published in Progress in Oceanography.

<sup>\*</sup> Corresponding author at: Key Laboratory of Marine Environment and Ecology, Ministry of Education, Ocean University of China, Qingdao 266100, China. *E-mail address:* hongjuc@ouc.edu.cn (H. Chen).

et al., 2008). The local hydrological structure and biogeochemistry process are potentially impacted by the pinch-off eddies' movement and energy transport (Ding and Jing, 2020; Itoh et al., 2014; Sasai et al., 2010). Mesoscale eddies and eddy fluxes that generate (such as vertical nutrient fluxes), which are essential to the dynamics of ocean circulation and the upper ocean ecosystems, have a significant impact on the distribution, community structure, and productivity of marine organisms (Duran-Campos et al., 2015; Goldthwait and Steinberg, 2008; Gómez et al., 2020; Landry et al., 2008; Nagai et al., 2015; Riquelme-Bugueño et al., 2015; Yebra et al., 2018).

Marine zooplankton are an essential component of the pelagic ecosystem, acting as a critical link between phytoplankton and higher trophic levels (Rocha-Díaz et al., 2021; Wassmann et al., 2006). They also play a vital role in marine carbon cycling and other ecological processes (Ge et al., 2021; Steinberg and Landry, 2017). Zooplankton have always been the main focus in the KE region (Ge et al., 2022; Komatsu et al., 2007; Lin et al., 2020; Morita et al., 2017; Shimode et al., 2012; Zang et al., 2023). A study by Komatsu et al. (2007) using a threedimensional ecosystem model revealed that the advective processes of the Kuroshio stream increased the biomass of phytoplankton and zooplankton in the KE region. Additionally, the advection of the Kuroshio stream can also transport warm-water and coastal species from southern Japan to the Kuroshio-Oyashio mixed water (KOMW) area (Chiba et al., 2009; Chiba et al., 2013; Miyamoto et al., 2022; Sogawa et al., 2019). Moreover, the plankton community in this area was also affected by the presence of rings pinched off from the KE stream. For instance, the concentration of chlorophyll (Chl) a increased when the cold-core rings pinched off from the KE, which was significantly higher than in the nearby subtropical waters (Nakano et al., 2013; Sasai et al., 2010). However, the specific impact of pinch-off rings on the zooplankton community in the KE area is unclear.

In recent years, functional traits have been increasingly used to assess and predict marine zooplankton community shifts along environmental and biological gradients (Barton et al., 2013; Benedetti et al., 2018; Brun et al., 2016). Brun et al. (2016) found that copepod body size was larger at high latitudes compared to low latitudes. Additionally, high-latitude regions were dominated by ambush-feeding copepods, while low latitudes exhibited a combination of ambushing and cruise-feeding copepods (Prowe et al., 2019). The functional traits of zooplankton are closely linked to various marine ecological and biogeochemical processes. For instance, zooplankton body size affects the fate of the primary production and determines the contributions of their fecal pellets to vertical material fluxes in the ocean (Barton et al., 2013; Stamieszkin et al., 2015; Turner, 2002). However, research on zooplankton functional traits in the KE region is still insufficient, and the effects of species-level trait variations on actual ecological and biogeochemical processes such as grazing and carbon export remain unclear.

We hypothesized that the KE jet altered zooplankton species composition and functional traits in the northwestern Pacific. Additionally, we expected that the pinch-off cyclonic eddy enhanced the nutrients and plankton biomass in the upper layers. In April 2015, the KE meandered southward between 144°E and 146°E, accompanied by a pinch-off cyclonic eddy. To investigate the impact of the KE jet and pinch-off eddy on zooplankton community structure and functional traits, we conducted an observational study during this period. Our research addressed two main questions: (1) Does the KE jet impede connectivity among zooplankton communities in the northwestern Pacific and affect local zooplankton biodiversity and functional traits? (2) What are the implications of the pinch-off cyclonic eddy on the distribution and biomass of zooplankton?

#### 2. Materials and Methods

#### 2.1. Study area

East of Japan, the KE meanders eastward within the subtropical gyre

of the North Pacific (Oiu, 2002). Typically, the sea surface temperature (SST) of the KE is warmer than its northern adjacent seas and comparable to that of its southern neighboring waters (Chen, 2008; Nishikawa and Yasuda, 2011; Xi et al., 2022). Furthermore, the Chl a concentration in the KE and its adjacent areas increases from lower to higher latitudes (Long et al., 2019). Strong cyclonic eddies are frequently observed in the south of the KE stream (Ding et al., 2019). Such cyclonic eddies primarily form when the southward meanders of the current pinch-off from the main current of the KE and are made up of cold fresh waters from the poleward side of the KE. Because the cold water becomes the core of the eddies, wrapped by warm water of the currents, they are known as coldcore eddies (Olson et al., 1980). Additionally, the pinch-off cold-core eddies exhibit characteristics of low salinity, high nutrients, and elevated Chl a concentrations compared to the surrounding seawater (Kouketsu et al., 2016; Nakano et al., 2013). The area between the KE and the Oyashio front is called the Kuroshio-Oyashio mixed water region, where the cold, low-salinity Oyashio waters encounter the warm, high-salinity subtropical Kuroshio waters, forming extremely complex oceanographic structures and a highly productive environment (Morita et al., 2017). South of the KE is the largest continuous biome on Earth-the North Pacific Subtropical Gyre (NPSG), where the surface waters are characterized by low nutrient content and phytoplankton growth (Suzuki et al., 1997; Zhang et al., 2012).

#### 2.2. Field sampling and laboratory processing

The research cruise was undertaken aboard the RV "Dong Fang Hong 2" along the transect of  $147^\circ$  E  $(30^\circ N{-}38^\circ N)$  within the northwestern Pacific from 10 April to 27 April 2015. The present study carried out a single observation along the transect. Upon reaching station B9 on April 10, sampling commenced in a south-to-north direction. Due to the unfavorable weather conditions between April 14 and April 24, sampling operations were temporarily suspended. On April 25, upon arrival at station B1, we continued sampling there from north to south, and we finished all of the sampling work on April 27 (Fig. 1). Zooplankton samples were procured by vertical tows with a WP-2 net (mouth area 0.25  $m^2$ , mesh size 200  $\mu m$ ), equipped with a calibrated flowmeter (Hydro-Bios Kiel, Germany). Towing was conducted from 200 m depth to the sea surface, at a speed of 0.8–1.0  $m\cdot s^{-1}$ . A total of 9 samples were collected, and zooplankton samples were preserved in a 4 % formalin-seawater solution immediately after each towing.

In the laboratory, zooplankton samples were analyzed and counted using a stereomicroscope (Leica S8APO, Germany). All adult zooplankton were identified to the species level when feasible, and pelagic larvae were identified to the taxa level. A subsample was obtained from each original sample using a Folsom plankton splitter, ensuring a minimum of 500 adult individuals were included, and the subsample volume was determined based on the density of organisms within the original sample. The data for each species only included adult individuals. For instance, only adult stage copepods (CVI) were included in the data for each copepod species, while immature individuals (copepodite CI to CV) were identified as copepodite larvae. The adult stages of macro- and mesozooplankton, like chaetognaths, were also identified and documented, while their larvae were recorded separately, such as Sagittidae larva. The wet weight biomass of the zooplankton was quantified using an analytical balance (SHPSI JA2003N, China). Zooplankton abundances and biomass were expressed in terms of individuals and wet weight per 1 m<sup>3</sup>. Red Noctiluca scintillans was excluded from the total abundance and was analyzed separately. Generally, N. scintillans is typically found in coastal waters (Harrison et al., 2011), whereas it bloomed (1.2  $\times$  10<sup>4</sup> ind·m<sup>-3</sup>) at station B3. Thus, *N. scintillans* was deemed an invasive species, and the effects of their bloom on the zooplankton community and functional traits were analyzed.

Vertical profiles of temperature and salinity were obtained from the sea surface to 200 m depth using a conductivity-temperature-density profiler (CTD) (Sea-Bird SBE 911, United States). In order to assess

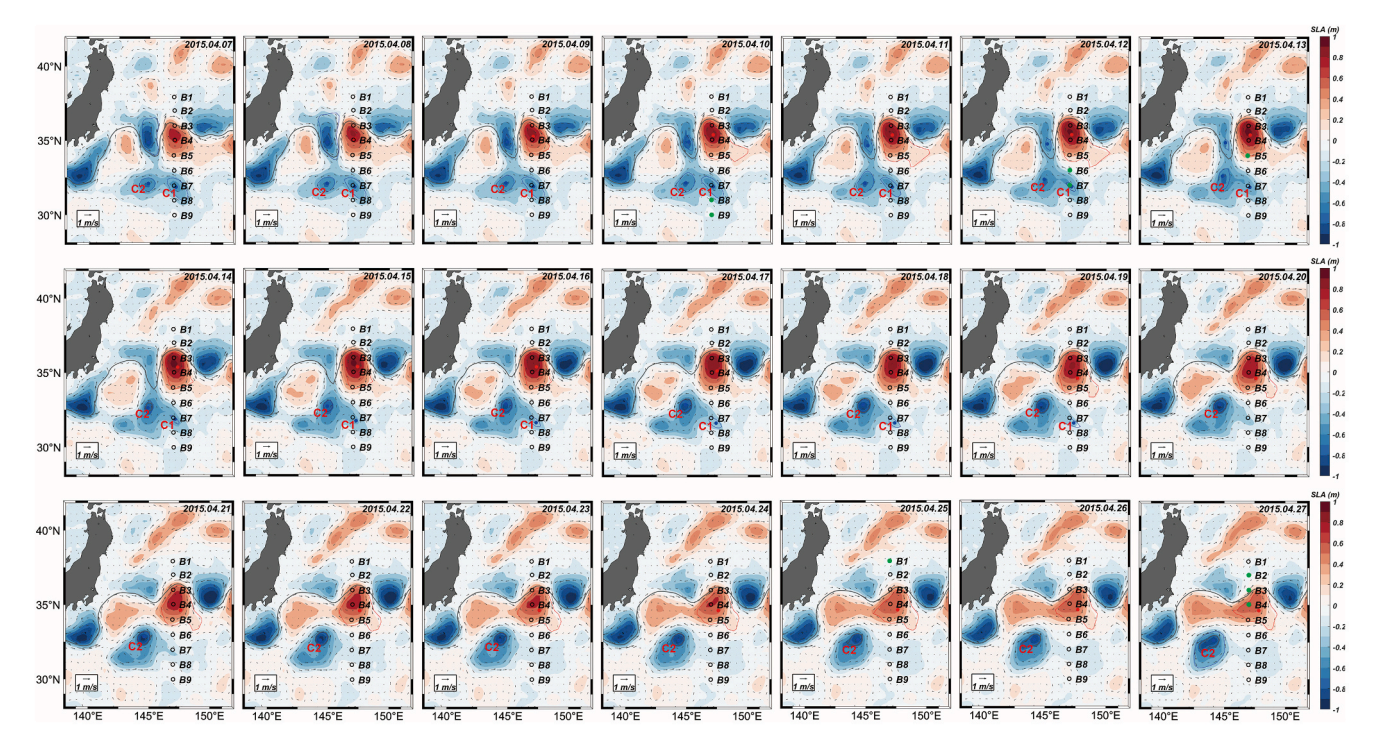


Fig. 1. The daily sea level anomaly (color shading) and surface geostrophic velocity anomalies (arrows) from 7 April to 27 April 2015. The sea level anomaly represented the deviation between the local sea level and the average sea level. The green dots denoted the stations where samples were collected on a particular day. The red and blue dots represented the core of anticyclonic and cyclonic eddies, respectively. The enclosed regions delineated by the red and blue lines indicate the central areas of the anticyclonic and cyclonic eddies correspondingly. C1 and C2 represented cyclonic eddies 1 and 2, respectively. The gray line represented the Kuroshio extension jet (0.9 m-ADT contour). (For interpretation of the references to color in this figure legend, the reader is referred to the web version of this article.)

nutrients (NO $_3$ -N, NO $_2$ -N, PO $_4$ -P and SiO $_3$ -Si) and Chl a concentration at specific depths (5 m, 25 m, deep chlorophyll maximum (DCM) layer, 100 m, 150 m, and 200 m), water samples above 200 m were collected by employing the acid-washed Teflon-coated Go-Flo bottles installed on the CTD system. The nutrient concentrations were analyzed using a nutrient automatic analyzer (SEAL Analytical, AutoAnalyzer 3, Germany) (Grasshoff et al., 2009). Furthermore, Chl a samples were filtered through 3  $\mu$ m and 0.2  $\mu$ m polycarbonate membranes (Millipore, United States) to estimate phytoplankton concentrations across different particle size ranges. Subsequently, all of Chl a samples were preserved in liquid nitrogen for further analysis. In the laboratory, Chl a samples underwent extraction in 90 % acetone for 24 h in the dark before being measured with a fluorescence photometer (F-4500, HITACHI, Japan).

#### 2.3. Data analysis

The data of daily sea level anomaly (SLA), surface geostrophic velocity anomalies (GVA), SST, and surface Chl a concentration were acquired from CMEMS (Copernicus-Marine Environment Monitoring Service, https://marine.copernicus.eu/). The SLA and GVA data were utilized to delineate the ocean surface current patterns within the study area. Furthermore, to supplement our comprehension of mesoscale eddies, the altimetric Mesoscale Eddy Trajectory Atlas product (Pegliasco et al., 2022) was utilized. This product was derived from satellite data provided by CMEMS and offered insights into mesoscale eddies, including their position, altitude, edge, and trajectory. Here, the speed contour was identified as the boundary of the mesoscale, representing the contour of the maximal circu-average speed of each mesoscale eddy. The path of the KE jet was defined by the 0.9 m Absolute Dynamic Topography (ADT) contour (Gentile et al., 2018; Zhang et al., 2022). The spatial resolutions of the SLA, GVA, SST, and satellite surface Chl a concentration data were  $0.25^{\circ} \times 0.25^{\circ}$ ,  $0.25^{\circ} \times 0.25^{\circ}$ ,  $0.083^{\circ} \times 0.083^{\circ}$  $0.083^{\circ}$ , and  $0.25^{\circ} \times 0.25^{\circ}$ , respectively.

The Shannon-Wiener index (H') and evenness index (J') were applied to assess the biodiversity of the zooplankton community. The Kdominance curve was utilized to visually exhibit the species richness and evenness of the zooplankton community, and was plotted using the PRIMER software (Dominance plot program). Additionally, the abundance data underwent log (x + 1) transformation and were utilized to construct a similarity matrix between stations based on the Bray-Curtis coefficient of similarity (Field et al., 1982). Station interrelations were clustered based on the average linkage group classification (Field et al., 1982). The similarity profile (SIMPROF) test and analysis of similarity (ANOSIM) were employed to assess the significantly dissimilar between clusters (Clarke, 1993). In pairwise comparisons, an R-statistic value close to 1 indicated a considerable difference. The RELATE test was applied to evaluate the correlation between zooplankton and environmental variables. Based on the abundance ranking of each species within their respective groups, the top three species were identified as the dominant species in each group. Multivariate analyses were conducted using the PRIMER software version 6 (PRIMER-E, United Kingdom).

Mean body length (mm), feeding type, trophic group, and reproductive mode were chosen as four functional traits of zooplankton that cover distinct and crucial ecological functions and may have an impact on the functioning of marine ecosystems (Benedetti et al., 2016; Kiørboe, 2011; Litchman et al., 2013). Body size, considered a "master trait", transcends and scales with various traits related to ecosystem processes, such as nutrient transfer, secondary productivity, and marine carbon cycling (Litchman et al., 2013). The mean body lengths of adult individuals were classified into four length types: < 1, 1–2, 2–5, and > 5 mm, representing small, medium, large, and giant zooplankton, respectively (Benedetti et al., 2016; Ge et al., 2022; Steinberg et al., 2008). Additionally, we examined the latitudinal variation of community-weighted mean (CWM) body lengths of zooplankton (Benedetti et al., 2022). Feeding type of organisms determine their prey selection, energy allocation, and nutrient cycling (Kiørboe, 2011).

Feeding types were classified into four categories: current feeding (CU), ambush feeding (AM), cruise feeding (CR), and mixed feeding (MI, for species capable of switching between two types) (Benedetti et al., 2016). We defined current and cruise feeding as active-feeding strategies, and ambush feeding as a passive-feeding mode (Kiørboe, 2011). The trophic group characterizes the primary food source of a species and, consequently, its role in food-web dynamics (Pomerleau et al., 2015). Trophic groups were classified into five types: omnivore (OM), omnivore-herbivore (O-H), carnivore (CA), omnivore-carnivore (O-C), and omnivore-detritivore (O-D) (Benedetti et al., 2018). Spawning strategy also influences the energy allocations organism (Litchman et al., 2013). Four types of egg-spawning strategies were identified: alternation of generation (AG), broadcast spawner (BS), sac spawner (SS), and binary fission (BF). Trait information was primarily obtained from previous studies (Barton et al., 2013; Benedetti et al., 2016; Brun et al., 2016; Chen and Shi, 2002; Deibel and Lowen, 2012; Pomerleau et al., 2015; Xu et al., 2014; Zheng et al., 1984 etc.) and online sources ((https://www. eol.org; https://copepodes.obs-banyuls.fr/en; see supporting information). Each species, except for pelagic larvae, was assigned trait types, forming a trait list (supporting information). The data on pelagic larvae were not included in the trait analysis since they were highly complicated and challenging to collect trait information (Krztoń and Kosiba,

Redundancy analysis (RDA) was employed to analyze the link between zooplankton and environmental parameters in various stations (Lepš and Šmilauer, 2003). The results of the RDA were visualized using CANOCO 5.0. Prior to analysis, all environmental variables and zooplankton abundance underwent log (x + 1) transformation. Explanatory variables included SST, sea surface salinity (SSS), Chl  $\alpha$  concentration, the temperature at 200 m depth (SBT), and salinity at 200 m depth (SBS). The differences in environment parameters, zooplankton abundance, and functional traits among distinct regions were compared using one-way ANOVA in SPSS 25 (IBM, United States). Prior to ANOVA, the Kolmogorov–Smirnov test was applied to check the normality of the zooplankton abundance.

#### 3. Results

#### 3.1. Environmental factors

The SLA and GVA findings indicated notable fluctuations in the KE throughout the observational period (Fig. 1). The KE stream exhibited a southward meandering trajectory between 144°E and 146°E, ultimately dissipating on April 20 in conjunction with the formation of a cold pinch-off cyclonic eddy to the south. Based on the GVA and vertical temperature and salinity profiles, the 9 stations were divided into four types (Figs. 1, 2, S1, and S2). Stations B1 and B2 were impacted by the KOMW, displaying lower temperature and salinity compared to other stations. Station B3, located near the KE stream, exhibited high surface temperature but low temperature at 200 m depth, indicating that the upper layer at this station was primarily influenced by the KE, while the deeper layer was influenced by KOMW (Figs. 2a and S2). Station B4 (147.03°E, 35.03°N), situated within an anticyclonic eddy that was not a pinch-off ring, had a notably higher temperature than its southern counterpart, Station B9 (147°E, 29.98°N), indicating a significant influence from the KE (Figs. 2a and S2). Stations B5-B9 were affected by the NPSG. The cyclonic eddy C1 formed in the NPSG region (30.5°N-33°N, 146.5°E-148°E) gradually diminished in size and intensity during the investigating period, eventually merging with cyclonic eddy C2 on April 21 (Fig. 1). Station B7 was situated in the center of the eddy C1, where the temperature and salinity of the entire water column above 200 m were highly homogeneous, while stations B6 and B8 were located at the edges (Figs. 1, S1, and S2). The daily SLA variations at stations B4/B7 and within the cores of anticyclonic eddy and cyclonic eddy C1 during the investigation period were shown in Fig. S3.

Stations B1 and B2, located within the KOMW region, exhibited low SSTs of 13.8 and 14.7 °C, respectively, while station B4 recorded a higher SST of 20.5 °C compared to the other stations, followed by station B9 (20.0 °C) at a lower latitude (Fig. 2a). Similar patterns were observed in the remote sensing SST data (Fig. S4). Although the vertical variation trend of temperature from the surface to 200 m at station B3 was similar to that of stations B1 and B2, the sea temperatures above 200 m of station B3 were significantly higher than that of stations B1 and B2 due to the influence of the KE (one-way ANOVA, P < 0.001). In addition, the SST and thermocline at station B7 were observed to be low and shallow in comparison to stations located along the edge of the eddy C1. The SSSs at B8 and B9 were higher than that at other stations, followed by station B4, while stations B1 and B2 exhibited low SSS (Figs. 2b and S2). Station B7, located in the center of the eddy C1, displayed lower salinity compared to stations B6 and B8, signifying the influence of low-salinity subarctic water during the pinch-off event (Fig. S2). Stations B1 and B2 exhibited considerably lower salinities above 200 m depth compared to the other stations (one-way ANOVA, P < 0.001), while station B4 displayed high salinity similar to those at stations B8 and B9 (Fig. 2b).

In comparison to other stations, station B1 exhibited the highest Chl a concentration in the upper layers (< 50 m), followed by station B5, while stations B7, B8, and B9 displayed low Chl a concentration (similar to the findings from remote sensing Chl a data; refer to Figs. 2d and S5). Except for stations B5 and B9, all stations below 100 m depth exhibited low Chl a concentration (< 0.1 mg·m<sup>-3</sup>). Station B1 within the KOMW region had the highest mean water column Chl a, whereas stations in the NPSG (except station B5) exhibited oligotrophic features (Fig. 2c). The proportion of phytoplankton with various cell sizes within total Chl a varied across different regions (Fig. 2c). In the KOMW region, the proportion of the 0.2–3  $\mu$ m size-fraction in total Chl a was similar to that of > 3  $\mu m$  size-fraction. At station B3, the 0.2–3  $\mu m$  and > 3  $\mu m$  sizefraction constituted 60 % and 40 % of the total Chl a, respectively, whereas at station B4, these fractions accounted for 37 % and 63 % of the total Chl  $\alpha$ . In the NPSG region, phytoplankton with a size of 0.2–3  $\mu$ m comprised 33 %–59 % of the total Chl a, while the > 3  $\mu$ m sizefraction accounted for 41 %-67 %.

Stations B1 and B2 exhibited elevated surface nitrate and phosphate concentrations (4.6–5.0  $\mu mol \cdot L^{-1}$  and 0.32–0.34  $\mu mol \cdot L^{-1}$ , respectively) in comparison to other regions, with station B3 following closely (1.9  $\mu mol \cdot L^{-1}$  and 0.23  $\mu mol \cdot L^{-1}$ , respectively). Station B4, influenced by the KE, had low nutrients that were comparable to those of oligotrophic station B9 (Figs. 2e, 2f, and S6). Furthermore, nutrient concentrations below 150 m at station B7, located in the core of eddy C1, were higher than those at the oligotrophic station B9 in the NPSG (Figs. 2e, 2f, and S6).

#### 3.2. Zooplankton community structure and functional traits

A total of 272 taxa of zooplankton were recorded in this study, with copepods, tunicates, and pelagic larvae (such as copepodite larva and cypris larva) being the three predominant categories (Table S1). Based on cluster analysis and SIMPROF test, four station groups were identified (Fig. 3a). Additionally, these classified groups exhibited significant differences in species compositions (one-way ANOSIM, R = 0.949, P < 0.001). Group 3 had the highest biodiversity, followed by Group 1, whereas Group 2 was the lowest (Table S2). The total abundance of Group 4 was significantly higher than that of other groups (one-way ANOVA, P < 0.05; Fig. 4a).

Group 1 was situated in the KOMW area (Fig. 3a). Within this group, copepods constituted the predominant proportion of the total zooplankton abundance (71 %–80 %), followed by tunicates (5 %–18 %) (Fig. 4a; Table S1). Moreover, the species richness of Group 1 ranged from 117 taxa to 120 taxa (Fig. 3b; Table S1). The average total abundance of zooplankton was 740.1  $\pm$  178.1 ind·m $^{-3}$  (Fig. 4a; Table S1). The copepod species *Clausocalanus furcatus*, *Oithona fallax*, and *Oncaea media* were the dominant species, with respective abundance of 102.9  $\pm$ 

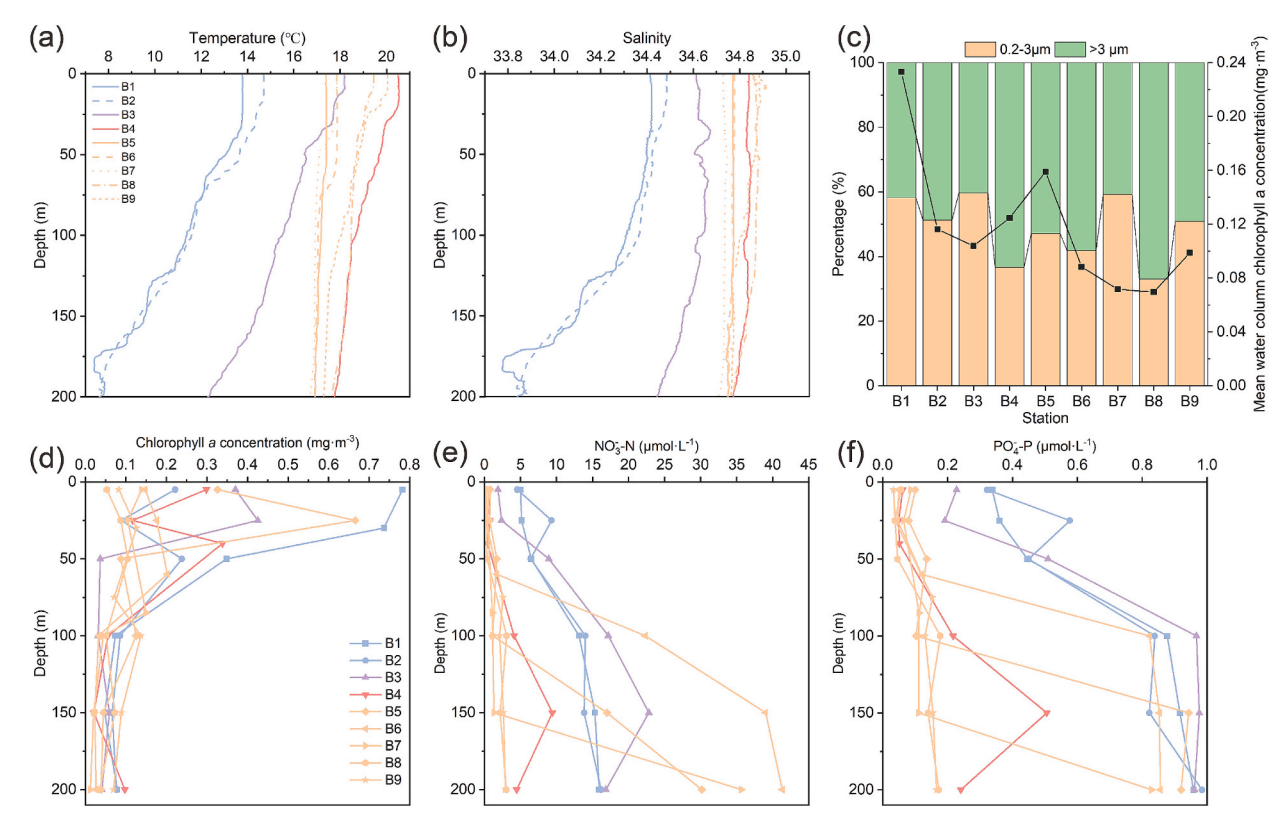


**Fig. 2.** Vertical profiles of temperature (a), salinity (b), chlorophyll *a* concentration (d), nitrate (e), and phosphate (f) above 200 m at each station. Blue, purple, red, and orange lines indicated that stations were influenced by Kuroshio-Oyashio mixed water, Kuroshio-Oyashio mixed water + Kuroshio Extension, Kuroshio Extension, and North Pacific Subtropical Gyre, respectively. Percentage composition of mean water column chlorophyll *a* concentration at each station (c). The black fold line represented the mean water column chlorophyll *a* concentration at each station.

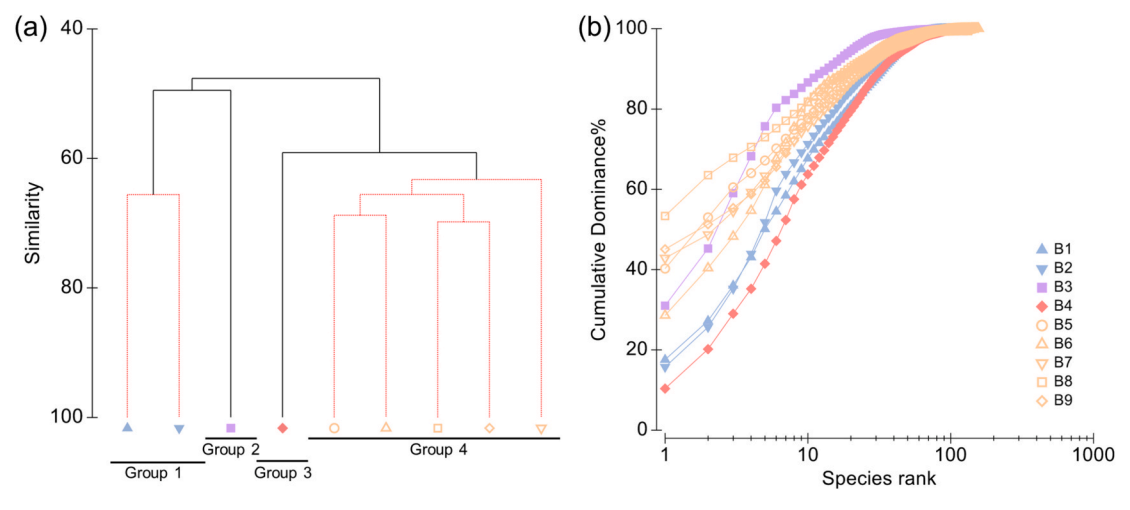


**Fig. 3.** The Cluster analysis and the SIMPROF test identified 4 groups of samples that are statistically distinct (a). The red dashed lines indicate groups of samples not separated by the SIMPROF test. *K*-dominance curves of zooplankton at each station (b). (For interpretation of the references to color in this figure legend, the reader is referred to the web version of this article.)

69.9, 66.1  $\pm$  25.0, and 54.6  $\pm$  8.9 ind·m<sup>-3</sup> (Table S3).

Group 2 was influenced by both the KOMW and KE. Similar to Group 1, copepods dominated the total zooplankton abundance (82 %), followed by tunicates (13 %) (Fig. 4a; Table S1). This group exhibited low species richness (95 taxa; Fig. 3b; Table S1), with a total abundance of 668.0 ind·m $^{-3}$  (Fig. 4a; Table S1). The copepod species *Paracalanus aculeatus*, *O. media*, and *Parvocalanus crassirostris* were the predominant species, with respective abundance of 207.3, 95.0, and 92.1 ind·m $^{-3}$  (Table S3). Additionally, a considerable quantity of cypris larvae (2.0

ind m<sup>-3</sup>), typically found in coastal regions, was detected within this group (see supporting information).

Group 3 was located within an anticyclonic eddy and impacted by the KE. A total of 137 taxa of zooplankton were recorded within this group (Fig. 3b; Table S1). Copepods accounted for 61 % of the total abundance, with pelagic larvae following in second at 19 % (Fig. 4a). The copepod species *Oithona plumifera* (50.6 ind·m<sup>-3</sup>), *O. fallax* (43.0 ind·m<sup>-3</sup>), and *Oncaea. venusta* (30.4 ind·m<sup>-3</sup>) were dominant within this group (Table S3). The total abundance of zooplankton was 488.5

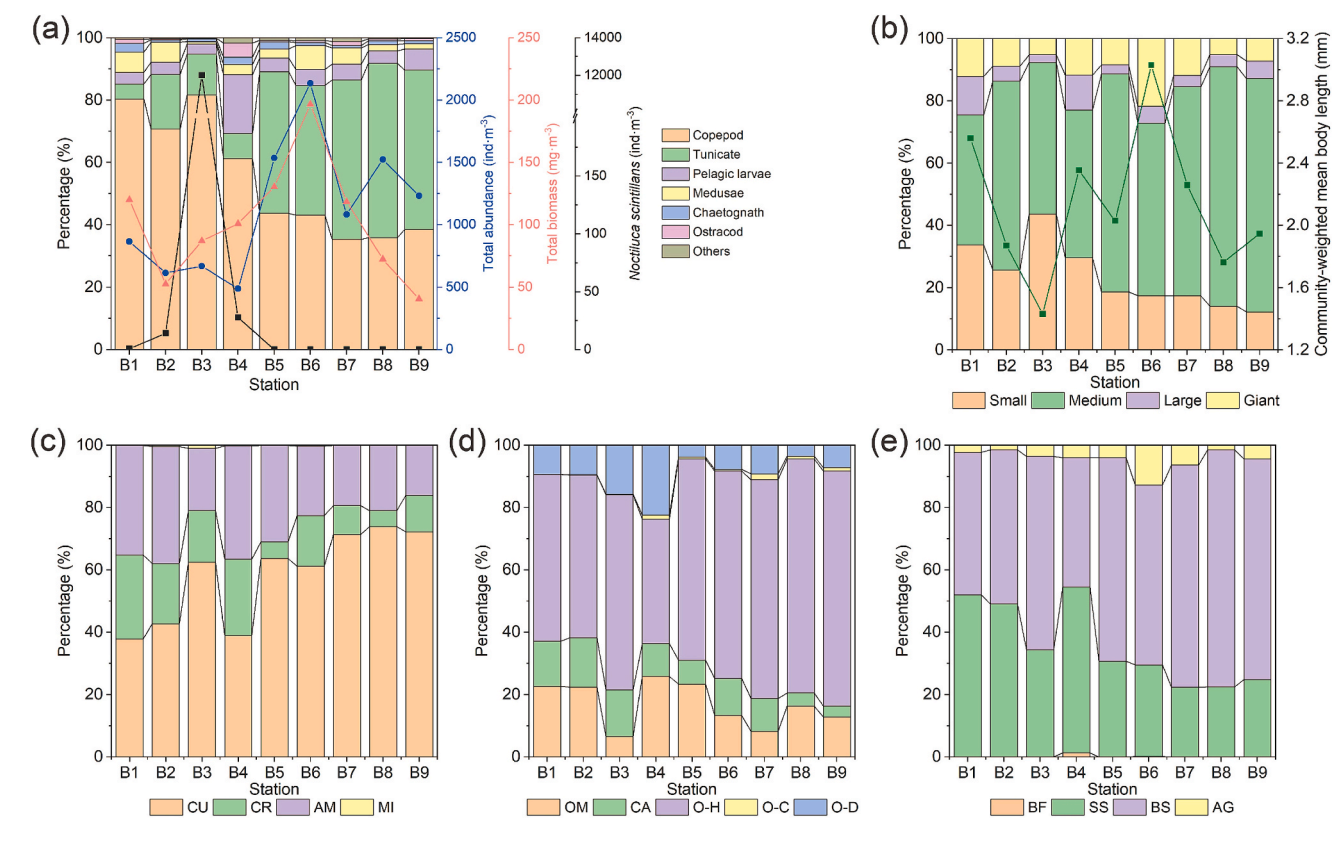


Fig. 4. Percentage of zooplankton abundance composition (a). The blue, red, and black fold lines represented the total abundance, total biomass, and *Noctiluca scintillans* at each station. Percentage of zooplankton body length (b). The green fold line represented the community-weighted mean body length of zooplankton at each station. Percentage of zooplankton feeding type (c), trophic group (d), and reproductive mode (e). (Small: < 1 mm; Medium: 1–2 mm; Large: 2–5 mm; Giant: > 5 mm; CU: current feeding; CR: cruise feeding; AM: ambush feeding; MI: mixed feeding; OM: omnivore; CA: carnivore; O–H: omnivore–herbivore; O–C: omnivore–carnivore; O–D: omnivore–detritivore; BF: binary fission; SS: sac spawner; BS: broadcast spawner; and AG: Alternation of generation). (For interpretation of the references to color in this figure legend, the reader is referred to the web version of this article.)

 $ind \cdot m^{-3}$  (Fig. 4a).

Group 4 encompassed a total of 5 stations and was impacted by the NPSG. Compared to other groups, this group had a higher species richness (137–157 taxa; Fig. 3b; Table S1). There was no significant difference in the species composition of zooplankton within the NPSG (P > 0.05). Tunicates (44 %–58 %) and copepods (37 %–46 %) constituted the majority of the overall abundance of zooplankton. *Fritillaria pellucida* (appendicularian), *O. plumifera* (copepod), and *Doliolum denticulatum* (doliolid) dominated in this group, which abundances were 612.6  $\pm$  127.7, 121.9  $\pm$  61.1, and 84.1  $\pm$  95.4 ind·m<sup>-3</sup>, respectively (Table S3). The mean total abundance of zooplankton was 1502.5  $\pm$  403.2 ind·m<sup>-3</sup>. Additionally, the total abundance of zooplankton at the center of pinchoff cyclonic eddy (station B7) was lower than at the edges (Fig. 4a).

N. scintillans was found in Groups 1–3, but was not detected within the Group 4 (Fig. 4a; Table S1). N. scintillans was most abundant at Station B3 ( $1.2 \times 10^4 \, \text{ind} \cdot \text{m}^{-3}$ ), followed by B4 and B2 ( $27.9 \, \text{and} \, 14.0 \, \text{ind} \cdot \text{m}^{-3}$ , respectively). At station B1, there were few N. scintillans ( $0.6 \, \text{ind} \cdot \text{m}^{-3}$ ) being found. N. scintillans bloomed at station B3, where its abundance was 18 times higher than the overall zooplankton abundance (Fig. 4a). Additionally, F. pellucida was abundant in Group 4 ( $464.6 \sim 813.0 \, \text{ind} \cdot \text{m}^{-3}$ ), and its maximum abundance was observed at station B8. However, F. pellucida was rare in Groups 2 and 3 ( $< 6.0 \, \text{ind} \cdot \text{m}^{-3}$ ) and not detected in Group 1.

The percentages of each single functional trait varied significantly among distinct groups (one-way ANOVA, P < 0.05), with the exception of feeding type (Fig. 4b-4e). Group 4 exhibited a higher percentage of medium zooplankton (55 %–77 %) in comparison to the other groups (41 %–48 %), while Group 2 exhibited a higher proportion (44 %) of small zooplankton (Fig. 4b). The proportions of large zooplankton were

the lowest across all groups. Additionally, station B6 exhibited the highest CWM body length of zooplankton compared to all other stations, with a high abundance of giant D. denticulatum, while the lowest CWM body length was observed at station B3 (Fig. 4b). When it comes to feeding types, each group was predominantly populated by current-feeding zooplankton (38 %-74 %), followed by ambush-feeding zooplankton (16 %-37 %), while mixed feeders accounted for a small percentage (< 1 %; Fig. 4c). Moreover, Group 4 exhibited a higher percentage of current feeders (61 %-74 %) compared to the other groups (excluding Group 2) (38 %-43 %). In terms of trophic groups, O-H zooplankton dominated the total abundance in each region (40 %-75 %), followed by omnivores (7 %-26 %), while O-C constituted the smallest fractions (< 2 %; Fig. 4d). The proportion of O-H in Group 4 (65 %–75 %) was higher than that in other groups (40 %–54 %), except for Group 2. The percentage of O-D was higher in Group 3 (22%) than in other groups (4 %–16 %), while Group 2 exhibited a lower proportion (7 %) of omnivores. In addition, broadcast spawners predominated in Groups 2 and 4 (58 %-76 %), whereas the percentage of sac spawners closely resembled that of broadcast spawners in Groups 1 and 3 (Fig. 4e).

#### 3.3. Correlation analyses between zooplankton and environmental factors

The RELATE analyses revealed a significant correlation between the zooplankton community and environmental variables (R=0.6, P<0.01). The results of RDA demonstrated that the first two canonical axes explained 79.6 % of the variation in the taxonomic composition of zooplankton. The first axis explained 65.4 % and was mostly negatively related to SBT; the second axis explained a further 14.2 % and was mostly negatively related to SSS (Fig. 5). Zooplankton total abundance,

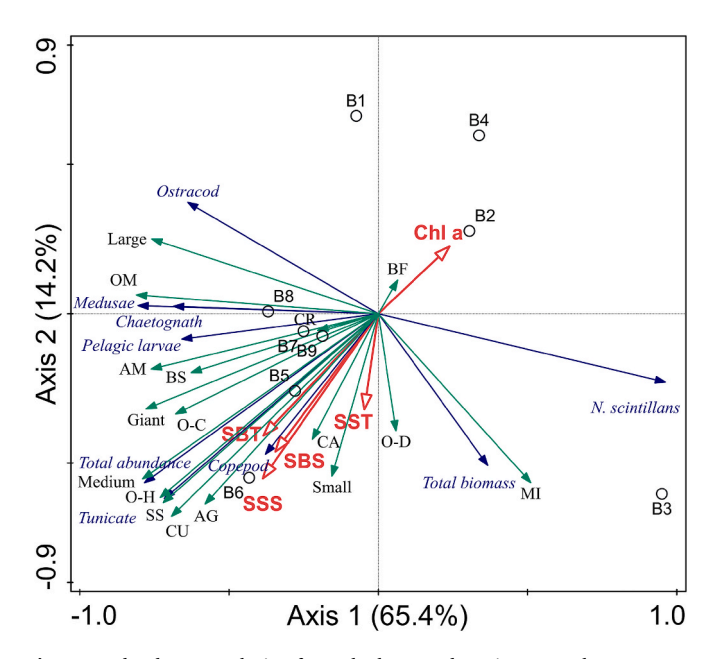


**Fig. 5.** Redundancy analysis of zooplankton and environmental parameters. SST, SSS, SBT, and SBS represented sea surface temperature, sea surface salinity, temperature at 200 m depth, and salinity at 200 m depth, respectively. Small, medium, large, and giant represented zooplankton with body lengths < 1 mm, 1–2 mm, 2–5 mm, and > 5 mm, respectively. CU, CR, AM, and MI represented current feeding, cruise feeding, ambush feeding, and mixed feeding, respectively. OM, CA, O–H, O–C, and O–D represented omnivore, carnivore, omnivore–herbivore, omnivore–carnivore, and omnivore–detritivore, respectively. BF, BS, SS, and AG represented binary fission, broadcast spawner, sac spawner, and alternation of generation, respectively.

copepods, and tunicates exhibited positive associations with SSS, SBT, and SBS. Medusae, chaetognaths, and pelagic larvae were positively associated with SBT and negatively associated with Chl a. Zooplankton biomass exhibited a positive association with SST. N. scintillans was positively associated with Chl a and negatively associated with SBT. In addition, MI and O–D zooplankton were positively associated with SST, while BF zooplankton exhibited a positive association with Chl a and a negative association with SST. Small and CA zooplankton displayed a positive association with SST and SSS, while medium, CU, O–H, SS, and AG zooplankton were positively associated with SBT, SBS, and SSS, and negatively associated with Chl a. The remaining traits of zooplankton exhibited a positive association with SBT.

#### 4. Discussions

#### 4.1. Differences in zooplankton community structure among regions

The zooplankton community formed a four-segment structure from north to south in the investigated regions. The KE acted as a barrier that prevented water exchange between the KOMW and NPSG (Figs. 3 and 6). Environmental variation among regions substantially affected zooplankton functional traits (Figs. 4 and 5), which were also widely recorded in global oceans (Barton et al., 2013; Brun et al., 2016; Corona et al., 2021; Heneghan et al., 2020; La Rosa-Izquierdo et al., 2022; Yebra et al., 2022). As for the "master trait" -body length, the warm NPSG region (Group 4) exhibited a much higher proportion of medium zooplankton (1-2 mm) in overall abundance compared to the stations influenced by KE and KOMW (Groups 1-3; Fig. 4b). The present study revealed a higher abundance of F. pellucida, which may explain the increased proportion of medium-sized zooplankton. F. pellucida is renowned for its rapid growth and reproduction capacity, as well as its capacity to adapt to high-temperature and high-salinity environments (Lopez-Urrutia et al., 2003). In this study, the pinch-off cyclonic eddy in the NPSG probably resulted in elevated primary production, which

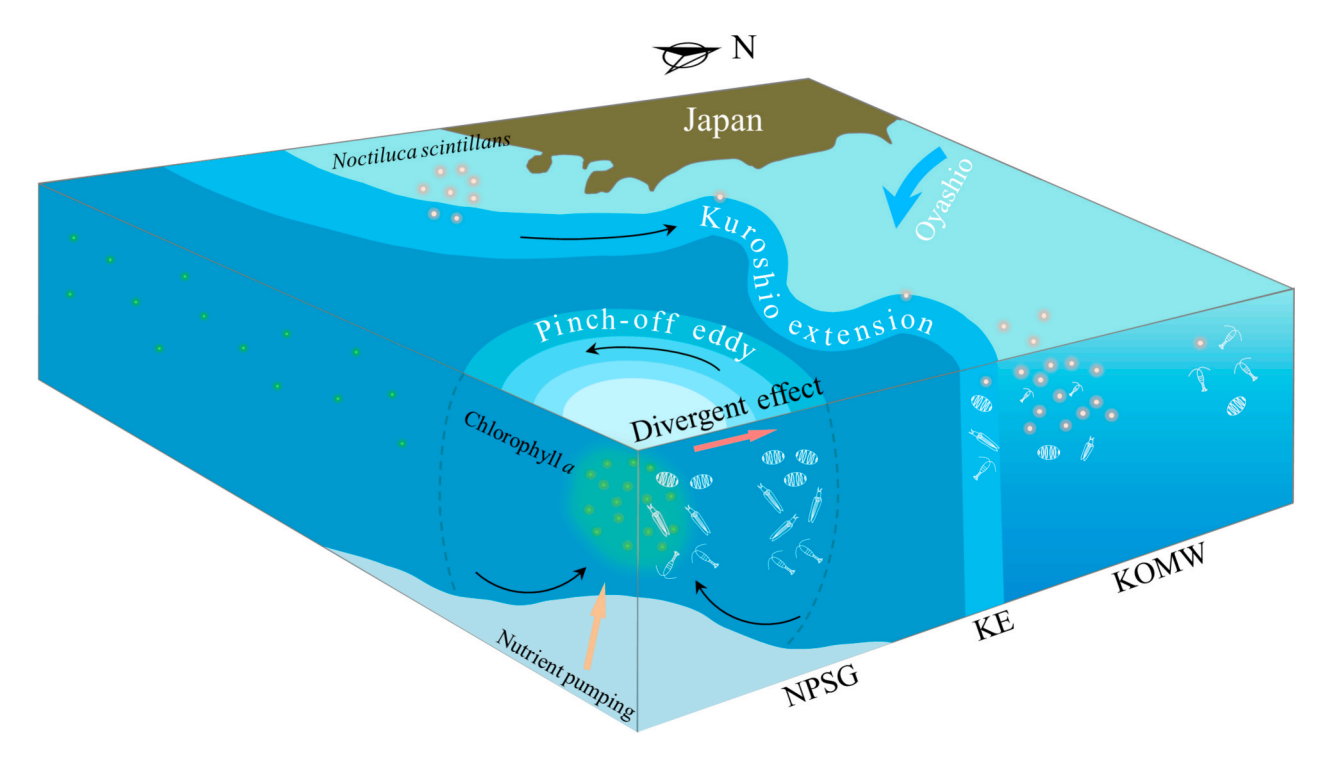


Fig. 6. Schematic illustration of the Kuroshio Extension (KE) jet and pinch-off eddy influence on zooplankton. The zooplankton communities constructed a zonal distribution, while the KE acted as a barrier that blocked water exchange between the Kuroshio-Oyashio mixed water (KOMW) and North Pacific Subtropical Gyre. N. scintillans was carried by the KE jet from the coast of Japan to the open sea, where it changed the local zooplankton community by blooming in the KOMW under favorable hydrological and nutritional environments. The pinch-off cyclonic eddy increased zooplankton abundance, and its divergent effect resulted in higher zooplankton abundance on the edges than within the center of the eddy.

likely contributed to the increased abundance of *F. pellucida*. Additionally, the high abundance of *F. pellucida* may have affected the composition of trophic groups in the NPSG region, as it accounted for more than 50 % of the O–H zooplankton. Consequently, the NPSG region (Group 4) exhibited a higher proportion of O–H zooplankton compared to the KOMW and KE regions (Groups 1–3).

Regarding feeding type, the KOMW region (Group 1) had a higher proportion of ambush-feeding zooplankton compared to other regions, while the NPSG region (Group 4) had a high proportion of current-feeding zooplankton. The variations in zooplankton feeding types among these regions likely reflect their trade-offs between resource acquisition, metabolic costs, and predation risks (Prowe et al., 2019). The ambush-feeding mode entails a lower encounter rate with prey, as well as reduced metabolic costs and predation risks, whereas the active-feeding mode represents the opposite (Kiørboe, 2011). In the relatively resource-rich KOMW region, ambush-feeding zooplankton might be able to acquire food with minimal metabolic costs while evading visual predators, thus leading to a higher proportion within the zooplankton community in this area (Kiørboe, 2011). However, due to the scarcity of resources in the NPSG region, most zooplankton increased prey encounter rates through active feeding in order to obtain more food to sustain their survival, despite the higher energy expenditure and increased vulnerability to predators (Ge et al., 2022). In addition, compared to the findings of Ge et al., this study suggested that the presence of the pinch-off cyclonic eddy in the NPSG may have substantially increased the proportion of current-feeding zooplankton. In contrast, the proportion of ambush-feeding zooplankton exhibited no significant change in this study. This could be attributed to the long period of reproductive cycles of ambush-feeding zooplankton such as some medusae and chaetognaths (Müller and Leitz, 2002; Uye and Liang, 2022), potentially resulting in their abundance changes lagging behind those of current feeders (Table S1).

## 4.2. N. scintillans bloom in the open ocean and its potential ecological effects

In the present study, red N. scintillans appeared in the KOMW and KE regions and bloomed at B3, where its abundance exceeded  $1.2 \times 10^4$ ind·m<sup>-3</sup>. Red N. scintillans is commonly found in temperate to subtropical coastal regions with temperatures ranging from about 10  $^{\circ}\text{C}$ to 25  $^{\circ}\text{C}$  and higher salinities (generally not in estuaries) (Harrison et al., 2011). The phenomenon of *N. scintillans* blooming in the KOMW region adjacent to the KE has remained unreported. This species occurs frequently in the coastal regions of southern Japan and is the primary causative organism of red tides in Japan on an annual basis (Harrison et al., 2011; Miyaguchi et al., 2006). Prior studies have indicated that the Kuroshio current can transport species from the coastal area of southern Japan to the KE and KOMW regions (Chiba et al., 2009; Chiba et al., 2013), and N. scintillans was recorded in the open sea of eastern Japan (141°E-145°E, 31°N-35°N; Nakata et al., 2004; Tomosada, 1984). In this study, N. scintillans from the nearshore coast of Japan may have been transported to station B3 by the KE jet during early-to-mid April. The southward swing of the KE stream (Fig. 1, 19 April to 27 April) resulted in station B3, which was previously exclusively impacted by the KE, being jointly influenced by the Kuroshio water and subarctic cold water, thus providing an ideal habitat for N. scintillans. It is worth noting that the occurrence of N. scintillans blooms in the KOMW areas adjacent to the KE may be a common yet underreported phenomenon. Additionally, cypris larvae, typically found in coastal regions (Anil et al., 2010; Weydmann-Zwolicka et al., 2021), were detected at station B3, possibly due to the Kuroshio advection. Station B2, on the other hand, may not be conducive to N. scintillans reproduction due to its low water temperature and distance from the KE stream.

*N. scintillans* is a common red tide organism whose bloom has been linked to severe harm to marine ecosystems (Quevedo et al., 1999; Umani et al., 2004). *N. scintillans* exhibits a broad range of body lengths,

typically between 0.2 and 2 mm, and possesses a voracious feeding behavior that enables it to consume a wide array of organisms, including fish eggs, phytoplankton, zooplankton, detritus, and bacteria. Competition for resources may impact on species that share similar food sources with N. scintillans (Quevedo et al., 1999; Ollevier et al., 2021). Batistic et al. (2019) have reported a notable decline in zooplankton abundance arising from the bloom of N. scintillans, given its restrictive effect on the food supply for zooplankton, particularly crustaceans. In this study, the bloom of N. scintillans might also affect the zooplankton community structure in the KOMW region. The zooplankton community at B3 differed significantly from that at adjacent stations B1 and B2: the community similarity was determined to be only 50 % (Fig. 3a), and the biodiversity of B3 was considerably lower than that of B1 and B2 (Fig. 3b). The abundance of small zooplankton such as C. furcatus, Oithona nana, and O. plumifera at station B3 decreased significantly compared to stations B1 and B2, potentially as a result of predation by N. scintillans. Furthermore, it is notable that the ecological efficiency within pelagic ecosystems correlates with the size spectra of plankton (du Pontavice et al., 2020; Sommer et al., 2002). Compared to stations B1 and B2, the shrinkage of zooplankton CWM body length at station B3, which was affected by the bloom of N. scintillans, might result in a decline in ecological efficiency.

The bloom of *N. scintillans* can potentially impact the marine carbon cycle and export. On the one hand, the ingestion and degradation of diatoms and copepod feces by N. scintillans impeded the sinking of particulate organic carbon to the deep layers of the ocean, thereby reducing the storage of CO<sub>2</sub> by biological pump (Kiørboe, 2003). Meanwhile, N. scintillans could reduce the abundance of some large and giant migrators by preying on their eggs and larvae to decrease their recruitment (Ollevier et al., 2021), subsequently influencing the contribution of the entire zooplankton community to active carbon flux. On the other hand, the vast array of metabolic products and carcasses generated during the bloom of N. scintillans may alter the carbon cycle within the microbial loop after being mineralized by bacteria (Vasas et al., 2007). Consequently, it is imperative to consider the impact of the N. scintillans bloom on the marine carbon cycle and export in the oligotrophic open ocean more comprehensively, necessitating further research in this region.

#### 4.3. Effects of pinch-off cyclonic eddy on zooplankton community

In general, cyclonic eddies pump deep seawater to the surface, and their centers typically exhibit characteristics of low temperature and high salinity (Kim et al., 2022; Li et al., 2021). However, in this study, the seawater temperature and salinity within the pinch-off cyclonic eddy were substantially lower compared to the surrounding area (Fig. 2). Remote sensing data indicated that the V-like meander of the KE from April 7th to April 16th, which was open towards the north, may have included low-salinity water from subarctic regions that infiltrated inside the meander before it closed (Fig. 1). Additionally, cyclonic eddies could replenish surface nutrients by pumping deep water, thereby promoting the growth of phytoplankton (Belkin et al., 2022; Guo et al., 2015; McGillicuddy et al., 2007). Similar findings were seen in this study where nutrient levels (at depths of 50-200 m) were higher within the eddy compared to the surrounding area (Fig. 2). However, the concentration of Chl a in the eddy did not exhibit a significant increase when compared to the adjacent area (station B9). The variation of Chl a is typically associated with the development stage of the cyclonic eddy, wherein Chl a level is significantly enhanced during the early stages, while Chl a level within the eddy center is not statistically distinguishable from the surrounding area during the later phase (McGillicuddy et al., 2007). Furthermore, the grazing activities of zooplankton can also lead to a reduction in Chl a concentration within the eddy (Landry et al., 2008). Thus, in this study, the low Chl a concentration within the eddy may be impacted by two aspects: (1) the eddy C1 was in the winding down phase and eventually dissipated on April 20th; and (2) the

increased abundance and grazing rates of zooplankton within the eddy (Goldthwait and Steinberg, 2008; Huggett, 2014).

Previous studies indicated that the zooplankton community in the NPSG region was characterized by high species richness and low abundance compared to the KOMW region (Sun and Wang, 2017; Zang et al., 2023). Meanwhile, copepods constituted the highest proportion (61 %) of total zooplankton abundance in the NPSG, followed by tunicates (14 %; Zang et al., 2023). However, unlike the early findings, the highest abundance of zooplankton occurred in the NPSG and tunicates were the dominant group in this study (Fig. 4a), which might be affected by the cyclonic eddy. Generally, the elevated Chl a associated with the cyclonic eddy can enhance the abundance of zooplankton, particularly O-H zooplankton species (Belkin et al., 2022; Decima and Landry, 2020). Abundant O-H tunicates were identified in this study, exhibiting significantly higher abundances than those reported by Zang et al. (2023). These tunicates, such as D. denticulatum and F. pellucida, are known to possess high clearance rates and potential population growth rates, enabling them to respond promptly to an increase in prey availability (Litchman et al., 2013). Furthermore, cluster analysis demonstrated a high degree of similarity in the zooplankton communities within the NPSG (Fig. 3a), suggesting a notable homogeneity in zooplankton taxonomic composition within this region. Differences in the zooplankton communities between the eddy and ambient region were primarily attributed to varying concentrations or dilutions of zooplankton, rather than extended isolation within the eddies (Huggett, 2014). Similar research findings have also been reported in the Mozambique Channel and adjacent waters of the Hawaiian Islands (Huggett, 2014; Landry et al., 2008). Notably, it was observed that the zooplankton abundance at station B7, situated at the center of the eddy, was noticeably lower than that at stations B6 and B8, located at the edges, owing to the divergent effects of cyclonic eddy processes (Hernández-León et al., 2001). The cyclonic eddy could promote zooplankton aggregation along the edges, resulting in higher abundance in these areas compared to the center (Goldthwait and Steinberg, 2008; Huggett, 2014; Rocha-Díaz et al., 2021).

Eddy-induced modifications in the structure and behavior of zooplankton communities may have crucial implications for the functioning of oligotrophic food webs and the transfer of particulate organic matter to deeper zones, consequently affecting carbon sequestration in the deep ocean (Eden et al., 2009; Goldthwait and Steinberg, 2008). In this study, variations in the zooplankton community driven by the pinch-off eddy in the NPSG region may affect marine carbon export. The heightened zooplankton biomass resulting from the pinch-off cyclonic eddy might potentially facilitate the export of particle organic carbon through the generation of abundant fecal pellets (Goldthwait and Steinberg, 2008). Moreover, the increased abundance of diel migrators (such as medusae and chaetognaths) contributed to an augmented active carbon flux into the deep ocean (Landry et al., 2008). Additionally, the substantial presence of tunicates within the cyclonic eddy may play a vital role in carbon export. Pelagic tunicates serve as current-feeding grazers, promoting the downward transport of carbon by producing a considerable quantity of particulate organic carbon detritus, including their "house" and fecal pellets (Flood et al., 1992; Luo et al., 2022). Further investigation is warranted to improve the understanding of the impacts of pinch-off cyclonic eddies on carbon export from zooplankton in the KE region and its adjacent areas.

Prior research has indicated significant seasonal variations in the hydrological environment of KE and its adjacent areas (Limsakul et al., 2001). Moreover, the meandering of the KE stream also displays seasonal fluctuations (Ding et al., 2019). However, this study only investigated a single transect across the KE and its adjacent areas during the spring season, and thus unable to reveal the seasonal variations in the zooplankton community of KE and its adjacent areas. Additionally, the different stages of the eddies may result in distinct patterns of zooplankton biomass and distribution (Goldthwait and Steinberg, 2008; Huggett, 2014). This study examined the influence of the later stage of

the cyclonic eddy on the zooplankton community. Consequently, the effects of the complete formation and dissipation processes of pinch-off cyclonic eddies on the zooplankton community remain unclear, warranting further investigation.

#### 5. Conclusion

The present study demonstrated the mesoscale variations of the zooplankton community in the KE region and its adjacent areas, clarifying the effects of the KE and pinch-off cyclonic eddies on zooplankton biodiversity and functional traits. Zooplankton communities across the KE and its adjacent regions exhibited a distinct four-segment pattern from north to south, with the KE functioning as a barrier that limited connectivity between zooplankton communities in the KOMW and NPSG regions. We documented a red N. scintillans bloom in the KOWM region adjacent to the KE stream and analyzed its potential effects on the zooplankton community and carbon export. This study constituted a case study, focusing on a single transect traversing the cyclonic eddy during its later phase. Despite the innovative revelation of the effects of the pinch-off cyclonic eddy in the KE region on plankton communities in this study, the broader ramifications of the complete formation and dissipation processes of pinch-off eddies on biogeochemical processes necessitate further investigation.

#### CRediT authorship contribution statement

Ruping Ge: Writing – review & editing, Writing – original draft, Formal analysis, Conceptualization. Hongju Chen: Writing – review & editing, Writing – original draft, Investigation, Funding acquisition, Formal analysis, Data curation, Conceptualization. Yueqi Zhang: Writing – review & editing, Formal analysis. Zhaohui Chen: Writing – review & editing, Funding acquisition. Facan Lei: Writing – original draft, Investigation. Weimin Wang: Writing – review & editing, Investigation, Formal analysis. Yunyun Zhuang: Writing – review & editing. Guangxing Liu: Writing – review & editing.

#### **Declaration of competing interest**

The authors declare that they have no known competing financial interests or personal relationships that could have appeared to influence the work reported in this paper.

#### Acknowledgement

This work was funded by the National Natural Science Foundation of China (No. 42076146, 41210008, 42225601). We thank Prof. Huiwang Gao from the College of Environmental Science and Engineering, Ocean University of China, and the crew members of the RV "Dong-Fang-Hong 2" for their assistance; We are grateful to Mr. Yousong Huang and Mr. Chenxi for their help in sample collection on board.

#### Appendix A. Supplementary data

Supplementary data to this article can be found online at https://doi.org/10.1016/j.pocean.2025.103523.

#### References

Anil, A., Khandeparker, L., Desai, D., Baragi, L., Gaonkar, C., 2010. Larval development, sensory mechanisms and physiological adaptations in acorn barnacles with special reference to Balanus amphitrite. J. Exp. Mar. Biol. Ecol. 392, 89–98.

Barton, A.D., Pershing, A.J., Litchman, E., Record, N.R., Edwards, K.F., Finkel, Z.V., Kiørboe, T., Ward, B.A., 2013. The biogeography of marine plankton traits. Ecol. Lett. 16, 522–534.

Batistic, M., Garic, R., Jasprica, N., Ljubimir, S., Mikus, J., 2019. Bloom of the heterotrophic dinoflagellate *Noctiluca scintillans* (Macartney) Kofoid & Swezy, 1921 and tunicates *Salpa fusiformis* Cuvier, 1804 and *Salpa maxima* Forskal, 1775 in the open southern Adriatic in 2009. J. Mar. Biol. Assoc. UK 99, 1049–1058.

- Belkin, N., Guy-Haim, T., Rubin-Blum, M., Lazar, A., Sisma-Ventura, G., Kiko, R., Morov, A., Ozer, T., Gertman, I., Herut, B., Rahav, E., 2022. Influence of cyclonic and anticyclonic eddies on plankton in the southeastern Mediterranean Sea during late summertime. Ocean Sci. 18, 693–715.
- Benedetti, F., Gasparini, S., Ayata, S., 2016. Identifying copepod functional groups from species functional traits. J. Plankton Res. 38, 159–166.
- Benedetti, F., Vogt, M., Righetti, D., Guilhaumon, F., Ayata, S., 2018. Do functional groups of planktonic copepods differ in their ecological niches? J. Biogeogr. 45, 604–616.
- Benedetti, F., Wydler, J., Vogt, M., 2022. Copepod functional traits and groups show divergent biogeographies in the global ocean. J. Biogeogr. 50, 8–22.
- Brun, P., Payne, M.R., Kiørboe, T., 2016. Trait biogeography of marine copepods an analysis across scales. Ecol. Lett. 19, 1403–1413.
- Chen, Q., Shi, C., 2002. Fauna Sinica, Invertebrata (Vol. 28), Phylum Arthropoda, Subphylum Crustacea, Order Amphipoda, Suborder Hyperiidea. Science Press, Beijing.
- Chen, S., 2008. The Kuroshio Extension front from satellite sea surface temperature measurements. J. Oceanogr. 64, 891–897.
- Chiba, S., Lorenzo, E.D., Davis, A., Keister, J.E., Taguchi, B., Sasai, Y., Sugisaki, H., 2013. Large-scale climate control of zooplankton transport and biogeography in the Kuroshio-Oyashio Extension region. Geophys. Res. Lett. 40, 5182–5187.
- Chiba, S., Sugisaki, H., Nonaka, M., Saino, T., 2009. Geographical shift of zooplankton communities and decadal dynamics of the Kuroshio-Oyashio currents in the western North Pacific. Global Change Biol. 15, 1846–1858.
- Clarke, K.R., 1993. Non-parametric multivariate analyses of changes in community structure. Austral Ecol. 18, 117–143.
- Corona, S., Hirst, A., Atkinson, D., Atkinson, A., 2021. Density-dependent modulation of copepod body size and temperature-size responses in a shelf sea. Limnol. Oceanogr. 66, 3916–3927.
- Decima, M., Landry, M., 2020. Resilience of plankton trophic structure to an eddystimulated diatom bloom in the North Pacific Subtropical Gyre. Mar. Ecol. Prog. Ser. 643, 33–48.
- Deibel, D., Lowen, B., 2012. A review of the life cycles and life-history adaptations of pelagic tunicates to environmental conditions. ICES J. Mar. Sci. 69, 358–369.
- Ding, Y., Jing, C., Qiu, Y., 2019. Temporal and spatial characteristics of pinch-off rings in the Kuroshio Extension region. Acta Oceanol. Sin. 41, 47–58.
- Ding, Y., Jing, C., 2020. Three-dimensional thermohaline anomaly structures of rings in the Kuroshio Extension region. Acta Oceanol. Sin. 39, 25–35.
- Duran-Campos, E., Salas-de-León, D.A., Monreal-Gómez, M.A., Aldeco-Ramírez, J., Coria-Monter, E., 2015. Differential zooplankton aggregation due to relative vorticity in a semi-enclosed bay. Estuar. Coast. Shelf S. 164, 10–18.
- Eden, B.R., Steinberg, D.K., Goldthwait, S.A., McGillicuddy, D.J., 2009. Zooplankton community structure in a cyclonic and mode-water eddy in the Sargasso Sea. Deep-Sea Res. PT I 56, 1757–1776.
- Field, J.G., Clarke, K.R., Warwick, R.M., 1982. A practical strategy for analysing multispecies distribution patterns. Mar. Ecol. Prog. Ser. 8, 37–52.
- Flood, P., Deibel, D., Morris, C., 1992. Filtration of colloidal melanin from sea-water by planktonic tunicates. Nature 355, 630–632.
- du Pontavice, H., Gascuel, D., Reygondeau, G., Maureaud, A., Cheung, W.W., 2020.
  Climate change undermines the global functioning of marine food webs. Global
  Change Biol. 26, 1306–1318.
- Ge, R., Chen, H., Zhuang, Y., Liu, G., 2021. Active carbon flux of mesozooplankton in South China Sea and western Philippine Sea. Front. Mar. Sci. 8, 697743.
- Ge, R., Li, Y., Chen, H., Lei, F., Zhuang, Y., Liu, G., 2022. Diel vertical distribution of mesozooplankton functional groups in the North Pacific Subtropical Gyre: A case study. Front. Mar. Sci. 9, 854642.
- Gentile, V., Pierini, S., de Ruggiero, P., Pietranera, L., 2018. Ocean modelling and altimeter data reveal the possible occurrence of intrinsic low-frequency variability of the Kuroshio Extension. Ocean Model. 131, 24–39.
- Goldthwait, S.A., Steinberg, D.K., 2008. Elevated biomass of mesozooplankton and enhanced fecal pellet flux in cyclonic and mode-water eddies in the Sargasso Sea. Deep-Sea Res. PT II 55, 1360–1377.
- Gómez, G., Nagai, T., Yokawa, K., 2020. Mesoscale warm-core eddies drive interannual modulations of swordfish catch in the Kuroshio Extension system. Front. Mar. Sci. 7, 680
- Grasshoff, K., Kremling, K., Ehrhardt, M., 2009. Methods of seawater analysis, 3rd completely revised and, enlarged edition. Willey, Weinheim.
- Guo, M., Chai, F., Xiu, P., Li, S., Rao, S., 2015. Impacts of mesoscale eddies in the South China Sea on biogeochemical cycles. Ocean Dynam. 65, 1335–1352.
- Hamilton, P., Lugo-Fernández, A., Sheinbaum, J., 2016. A loop current experiment: Field and remote measurements. Dynam. Atmos. Oceans 76, 156–173.
- Harrison, P., Furuya, K., Glibert, P., Xu, J., Liu, H., Yin, K., Lee, J., Anderson, D., Gowen, R., Al-Azri, A., Ho, A., 2011. Geographical distribution of red and green Noctiluca scintillans. Chin. J. Oceanol. Limn. 29, 807–831.
- Heneghan, R.F., Everett, J.D., Sykes, P., Batten, S.D., Edwards, M., Takahashi, K., Suthers, I.M., Blanchard, J.L., Richardson, A.J., 2020. A functional size-spectrum model of the global marine ecosystem that resolves zooplankton composition. Ecol. Model. 435, 109265.
- Hernández-León, S., Almeida, C., Gómez, M., Torres, S., Montero, I., Portillo-Hahnefeld, A., 2001. Zooplankton biomass and indices of feeding and metabolism in island-generated eddies around Gran Canaria. J. Marine Syst. 30, 51–66.
- Huggett, J.A., 2014. Mesoscale distribution and community composition of zooplankton in the Mozambique Channel. Deep-Sea Res. PT II 100, 119–135.
- Itoh, S., Yasuda, I., Úeno, H., Suga, T., Kakehi, S., 2014. Regeneration of a warm anticyclonic ring by cold water masses within the western subarctic gyre of the North Pacific. J. Oceanogr. 70, 211–223.

- Kim, D., Lee, S., Cho, S., Kang, D., Park, G., Kang, S.K., 2022. Mesoscale eddy effects on sea-air CO<sub>2</sub> fluxes in the northern Philippine Sea. Front. Mar. Sci. 9, 970678.
- Kiørboe, T., 2003. High turnover rates of copepod fecal pellets due to Noctiluca scintillans grazing. Mar. Ecol. Prog. Ser. 258, 181–188.
- Kiørboe, T., 2011. How zooplankton feed: mechanisms, traits and trade-offs. Biol. Rev. 86, 311–339.
- Komatsu, K., Matsukawa, Y., Nakata, K., Ichikawa, T., Sasaki, K., 2007. Effects of advective processes on planktonic distributions in the Kuroshio region using a 3-D lower trophic model and a data assimilative OGCM. Ecol. Model. 202, 105–119.
- Kouketsu, S., Kaneko, H., Okunishi, T., Sasaoka, K., Itoh, S., Inoue, R., Ueno, H., 2016. Mesoscale eddy effects on temporal variability of surface chlorophyll a in the Kuroshio Extension. J. Oceanogr. 72, 439–451.
- Krztoń, W., Kosiba, J., 2020. Variations in zooplankton functional groups density in freshwater ecosystems exposed to cyanobacterial blooms. Sci. Total Environ. 730, 139044.
- La Rosa-Izquierdo, Y., Hernandez-Trujillo, S., Aceves-Medina, G., 2022. Changes in the structure of the epipelagic copepod community on the western coast of the Baja California Peninsula before and during El Niño 2015. Mar. Biodivers. 52, 64.
- Landry, M.R., Decima, M., Simmons, M.P., Hannides, C.C., Daniels, E., 2008.
  Mesozooplankton biomass and grazing responses to Cyclone Opal, a subtropical mesoscale eddy. Deep-Sea Res. PT II 55, 1378–1388.
- Lepš, J., Šmilauer, P., 2003. Multivariate analysis of ecological data using CANOCO. Cambridge University Press, Cambridge.
- Li, R., Xu, J., Cen, X., Zhong, W., Liao, J., Shi, Z., Zhou, S., 2021. Nitrate fluxes induced by turbulent mixing in dipole eddies in an oligotrophic ocean. Limnol. Oceanogr. 66, 2842–2854
- Limsakul, A., Saino, T., Midorikawa, T., Goes, J., 2001. Temporal variations in lower trophic level biological environments in the northwestern North Pacific Subtropical Gyre from 1950 to 1997. Prog. Oceanogr. 49, 129–149.
- Lin, P., Ma, J., Chai, F., Xiu, P., Liu, H., 2020. Decadal variability of nutrients and biomass in the southern region of Kuroshio Extension. Prog. Oceanogr. 188, 102441.
- Lipphardt, B., Poje, A., Kirwan, A., Kantha, L., Zweng, M., 2008. Death of three Loop Current rings. J. Mar. Res. 66, 25–60.
- Litchman, E., Ohman, M.D., Kiørboe, T., 2013. Trait-based approaches to zooplankton communities. J. Plankton Res. 35, 473–484.
- Long, Y., Zhu, X., Guo, X., Huang, H., 2019. Temporal variation of Kuroshio nutrient stream south of Japan. J. Geophys. Res-Oceans 123, 7896–7913.
- Lopez-Urrutia, A., Irigoien, X., Acuna, J., Harris, R., 2003. In situ feeding physiology and grazing impact of the appendicularian community in temperate waters. Mar. Ecol. Prog. Ser. 252, 125–141.
- Luo, Y., Stock, A., Henschke, N., Dunne, P., O'Brien, D., 2022. Global ecological and biogeochemical impacts of pelagic tunicates. Prog. Oceanogr. 205, 102822.
- McGillicuddy, D., Anderson, L., Bates, N., Bibby, T., Buesseler, K., Carlson, C., Davis, C., Ewart, C., Falkowski, P., Goldthwait, S., Hansell, D., Jenkins, W., Johnson, R., Kosnyrev, V., Ledwell, J., Li, Q., Siegel, D., Steinberg, D., 2007. Eddy/wind interactions stimulate extraordinary mid-ocean plankton blooms. Science 316, 1021–1026.
- Miyaguchi, H., Fujiki, T., Kikuchi, T., Kuwahara, V., Toda, T., 2006. Relationship between the bloom of *Noctiluca scintillans* and environmental factors in the coastal waters of Sagami Bay. Japan. J. Plankton Res. 28, 313–324.
- Miyamoto, H., Takahashi, K., Kuroda, H., Watanabe, T., Taniuchi, Y., Kuwata, A., Kasai, H., Kakehi, S., Fuji, T., Suyama, S., Tadokoro, K., 2022. Copepod community structure in the transition region of the North Pacific Ocean: Water mixing as a key driver of secondary production enhancement in subarctic and subtropical waters. Prog. Oceanogr. 207, 102865.
- Morita, H., Toyokawa, M., Hidaka, K., Nishimoto, A., Sugisaki, H., Kikuchi, T., 2017. Spatio-temporal structure of the jellyfish community in the transition zone of cold and warm currents in the northwest Pacific. Plankton Benthos Res. 12, 266–284.
- Müller, W., Leitz, T., 2002. Metamorphosis in the Cnidaria. Can. J. Zool. 80, 1755–1771. Nagai, T., Gruber, N., Frenzel, H., Lachkar, Z., McWilliams, J., Plattner, G., 2015.
- Dominant role of eddies and filaments in the offshore transport of carbon and nutrients in the California Current System. J. Geophys. Res-Oceans 120, 5318–5341.
- Nagai, T., Durán, G., Otero, D., Mori, Y., Yoshie, N., Ohgi, K., Hasegawa, D., Nishina, A., Kobari, T., 2019. How the Kuroshio Current delivers nutrients to sunlit layers on the continental shelves with aid of near-inertial waves and turbulence. Geophys. Res. Lett. 46, 6726–6735.
- Nagai, T., Quintana, G., Gomez, G., Hashihama, F., Komatsu, K., 2021. Elevated turbulent and double-diffusive nutrient flux in the Kuroshio over the Izu Ridge and in the Kuroshio Extension. J. Oceanogr. 77, 55–74.
- Nakano, H., Tsujino, H., Sakamoto, K., 2013. Tracer transport in cold-core rings pinched off from the Kuroshio Extension in an eddy-resolving ocean general circulation model. J. Geophys. Res-Oceans 118, 5461–5488.
- Nakata, K., Itoh, H., Ichikawa, T., Sasaki, K., 2004. Seasonal changes in the reproduction of three oncaeid copepods in the surface layer of the Kuroshio Extension. Fish. Oceanogr. 13, 21–33.
- Nishikawa, H., Yasuda, I., 2011. Long-term variability of winter mixed layer depth and temperature along the Kuroshio jet in a high-resolution ocean general circulation model. J. Oceanogr. 67, 503–518.
- Ollevier, A., Mortelmans, J., Aubert, A., Deneudt, K., Vandegehuchte, M.B., 2021. *Noctiluca scintillans*: Dynamics, size measurements and relationships with small softbodied plankton in the Belgian part of the North Sea. Front. Mar. Sci. 8, 777999.
- Olson, D., 1980. The physical oceanography of two rings observed by the Cyclonic Ring Experiment, part II: Dynamics. J. Phys. Oceanogr. 10, 514–527.
- Pegliasco, C., Busché, C., Faugère, Y., 2022. Mesoscale Eddy Trajectory Atlas META3.2 Delayed-Time all satellites: version META3.2 DT allsat. https://doi.org/10.24400/527896/A01-2022.005.220209.

- Pomerleau, C., Sastri, A.R., Beisner, B.E., 2015. Evaluation of functional trait diversity for marine zooplankton communities in the Northeast subarctic Pacific Ocean. J. Plankton Res. 37, 712–726.
- Prowe, A., Visser, A., Andersen, K., Chiba, S., Kiorboe, T., 2019. Biogeography of zooplankton feeding strategy. Limnol. Oceanogr. 64, 661–678.
- Qiu, B., 2002. The Kuroshio Extension system: Its large-scale variability and role in the midlatitude ocean-atmosphere interaction. J. Oceanogr. 58, 57–75.
- Qiu, B., 2003. Kuroshio extension variability and forcing of the Pacific decadal oscillations: Responses and potential feedback. J. Phys. Oceanogr. 33, 2465–2482.
- Quevedo, M., Gonzalez-Quiros, R., Anadon, R., 1999. Evidence of heavy predation by Noctiluca scintillans on Acartia clausi (Copepoda) eggs off the central Cantabrian coast (NW Spain). Oceanologica Acta 22, 127–131.
- Riquelme-Bugueño, R., Correa-Ramírez, M., Escribano, R., Núñez, S., Hormazábal, S., 2015. Mesoscale variability in the habitat of the Humboldt Current krill, spring 2007. J. Geophys. Res-Oceans 120, 2769–2783.
- Rocha-Díaz, F.A., Monreal-Gómez, M.A., Coria-Monter, E., Salas-de-León, D.A., Durán-Campos, E., Merino-Ibarra, M., 2021. Copepod abundance distribution in relation to a cyclonic eddy in a coastal environment in the southern Gulf of California. Cont. Shelf Res. 222, 104436.
- Sasai, Y., Richards, K., Shida, A., Sasaki, H., 2010. Effects of cyclonic mesoscale eddies on the marine ecosystem in the Kuroshio Extension region using an eddy-resolving coupled physical-biological model. Ocean Dynam. 60, 693–704.
- Shimode, S., Takahashi, K., Shimizu, Y., Nonomura, T., Tsuda, A., 2012. Distribution and life history of two planktonic copepods, *Rhincalanus nasutus* and *Rhincalanus rostrifrons*, in the northwestern Pacific Ocean. Deep-Sea Res. PT I 65, 133–145.
- Sogawa, S., Hidaka, K., Kamimura, Y., Takahashi, M., Saito, H., Okazaki, Y., Shimizu, Y., Setou, T., 2019. Environmental characteristics of spawning and nursery grounds of Japanese sardine and mackerels in the Kuroshio and Kuroshio Extension area. Fish. Oceanogr. 28, 454–467.
- Sommer, U., Stibor, H., Katechakis, A., Sommer, F., Hansen, T., 2002. Pelagic food web configurations at different levels of nutrient richness and their implications for the ratio fish production: primary production. Hydrobiologia 484, 11–20.
- Stamieszkin, K., Pershing, A.J., Record, N.R., Pilskaln, C.H., Dam, H.G., Feinberg, L.R., 2015. Size as the master trait in modeled copepod fecal pellet carbon flux. Limnol. Oceanogr. 60, 2090–2107.
- Steinberg, D.K., Cope, J.S., Wilson, S.E., Kobari, T., 2008. A comparison of mesopelagic mesozooplankton community structure in the subtropical and subarctic North Pacific Ocean. Deep-Sea Res. PT II 55, 1615–1635.
- Steinberg, D.K., Landry, M.R., 2017. Zooplankton and the ocean carbon cycle. Annu. Rev. Mar. Sci. 9, 413–444.
- Sun, D., Wang, C., 2017. Latitudinal distribution of zooplankton communities in the Western Pacific along 160°E during summer 2014. J. Marine Syst. 169, 52–60.
- Suzuki, K., Handa, N., Kiyosawa, H., Ishizaka, J., 1997. Temporal and spatial distribution of phytoplankton pigments in the Central Pacific Ocean along 175°E during the boreal summers of 1992 and 1993. J. Oceanogr. 53, 383–396.
- Tomosada, A., 1984. Fronts accompanying the Kuroshio and warm core eddy related fisheries. Bulletin on Coastal Oceanography 21, 129–138 in Japanese.
- Turner, J.T., 2002. Zooplankton fecal pellets, marine snow and sinking phytoplankton blooms. Aquat. Microb. Ecol. 27, 57–102.

- Umani, S., Beran, A., Parlato, S., Virgilio, D., Zollet, T., De Olazabal, A., Lazzarini, B., Cabrini, M., 2004. Noctiluca scintillans MACARTNEY in the Northern Adriatic Sea: long-term dynamics, relationships with temperature and eutrophication, and role in the food web. J. Plankton Res. 26, 545–561.
- Usui, N., Tsujino, H., Nakano, H., Matsumoto, S., 2013. Long-term variability of the Kuroshio path south of Japan. J. Oceanogr. 69, 647–670.
- Uye, S., Liang, D., 2022. Seasonal population dynamics, production, and feeding of the chaetognath Aidanosagitta crassa in a temperate eutrophic inlet. Plankton Benthos Res. 17, 312–326.
- Vasas, V., Lancelot, C., Rousseau, V., Jordan, F., 2007. Eutrophication and overfishing in temperate nearshore pelagic food webs: a network perspective. Mar. Ecol. Prog. Ser. 336, 1–14
- Wassmann, P., Reigstad, M., Haug, T., Rudels, B., Carroll, M.L., Hop, H., Gabrielsen, G. W., Falk-Petersen, S., Denisenko, S.G., Arashkevich, E., Slagstad, D., Pavlova, O., 2006. Food webs and carbon flux in the Barents Sea. Prog. Oceanogr. 71, 232–287.
- Weydmann-Zwolicka, A., Balazy, P., Kuklinski, P., Soreide, J., Patu, W., Ronowicz, M., 2021. Meroplankton seasonal dynamics in the high Arctic fjord: Comparison of different sampling methods. Prog. Oceanogr. 190, 102484.
- Xi, J., Wang, Y., Feng, Z., Liu, Y., Guo, X., 2022. Variability and intensity of the sea surface temperature front associated with the Kuroshio Extension. Front. Mar. Sci. 9, 836469
- Xu, Z., Huang, J., Lin, M., Guo, D., Wang, C., 2014. The Superclass Hydrozoa of the Phylum Cnidaria in China. Ocean Press, Beijing.
- Yamamoto, T., Nishizawa, S., Taniguchi, A., 1988. Formation and retention mechanisms of phytoplankton peak abundance in the Kuroshio front. J. Plankton Res. 10, 1113–1130
- Yang, H., Guo, X., Miyazawa, Y., Varlamov, S.M., Abe-Ouchi, A., Chan, L., 2022. Changes in the Kuroshio path, surface velocity and transport during the last 35,000 years. Geophys. Res. Lett. 49, e2021GL097250.
- Yebra, L., Herrera, I., Mercado, J.M., Cortes, D., Gomez-Jakobsen, F., Alonso, A., Sanchez, A., Salles, S., Valcarcel-Perez, N., 2018. Zooplankton production and carbon export flux in the western Alboran Sea gyre (SW Mediterranean). Prog. Oceanogr. 167, 64–77.
- Yebra, L., Puerto, M., Valcarcel-Perez, N., Putzeys, S., Gomez-Jakobsen, F., Garcia-Gomez, C., Mercado, J.M., 2022. Spatio-temporal variability of the zooplankton community in the SW Mediterranean 1992-2020: Linkages with environmental drivers. Proc. Oceanogr. 203. 102782.
- Zang, Y., Chen, H., Zhuang, Y., Ge, R., Wang, W., Liu, G., 2023. Latitudinal transition of epipelagic mesozooplankton in the northwestern Pacific in winter. Mar. Environ. Res. 186, 105915.
- Zhang, D., Wang, C., Liu, Z., Xu, X., Wang, X., Zhou, Y., 2012. Spatial and temporal variability and size fractionation of chlorophyll a in the tropical and subtropical Pacific Ocean. Acta Oceanol. Sin. 31, 120–131.
- Zhang, Y., Yu, W., Chen, X., Zhou, M., Zhang, C., 2022. Evaluating the impacts of mesoscale eddies on abundance and distribution of neon flying squid in the Northwest Pacific Ocean. Front. Mar. Sci. 9, 862273.
- Zheng, Z., Li, S., Xu, Z., 1984. Marine planktology. Ocean Press, Beijing.